Numerical modeling of the electromagnetic coupling effects for phase error correction in EIT borehole measurement

Y Zhao[1], E Zimmermann[1], J A Huisman[2], A Treichel[2], B Wolters[1], S van Waasen[1]
[1]Central Institute ZEA-2 – Electronic Systems,
[2]Institute of Bio- and Geosciences IBG-3 - Agrosphere
Forschungszentrum Juelich GmbH
52425 Juelich, Germany

A Kemna[3]
[3]Department of Geodynamics and Geophysics
University of Bonn
53115 Bonn, Germany

***Abstract*— Electrical Impedance Tomography (EIT) applications in geophysics require long electrode chains (25 m) for current injection and potential measurements. Undesired inductive coupling between the wire loops for current injection and potential measurement and capacitive coupling between the cable shield and the soil strongly decrease the phase accuracy of such measurements for frequencies above 100 Hz. Therefore, the bandwidth of EIT field measurements is typically limited to the mHz to Hz range. To overcome this limitation, we derived correction procedures for inductive and capacitive coupling by combining numerical modeling with calibration measurements. The correction procedures were verified with test measurements, where a phase accuracy better than 1 mrad at 10 kHz was achieved.**

I. INTRODUCTION

Spectral Electrical Impedance Tomography (EIT) allows obtaining images of the complex electrical conductivity of objects for a broad frequency range from mHz to kHz [2]. It has recently received increased interest in the field of near-surface geophysics because of the relationships between complex electrical properties and hydrogeological and biogeochemical properties observed in the laboratory with Spectral Induced Polarization (SIP) [1]. However, these laboratory results indicate that a high phase accuracy is required because many soils and sediments are only weakly polarizable and show small phase angles between 1 and 20 mrad only [4]. It is a challenge to reach this phase accuracy in a broad frequency range for EIT field measurements based on the developments in [7].

For the field application, the existing EIT laboratory system [7] was extended with borehole logging tools and electrode chains where long cables (25 m) are used to attach the electrodes. Such long cables can lead to substantial inductive coupling between the electric loops for current injection and potential measurement. The measured phase may also be affected by capacitive coupling between the cable and the electrically conductive environment. Both types of coupling can cause large phase errors that have typically limited the bandwidth of field EIT measurements to the mHz to Hz range. In this work, we will derive correction methods for inductive coupling effects in order to improve the phase accuracy of EIT measurements in one borehole. In contrast to previous work [6], we here use a new pole-pole calibration measurement. The newly proposed correction procedure will be validated using measurements under controlled conditions. Finally, an application to real field measurements will be shown.

This research is supported by the project "4D Electrical Impedance Tomography" funded by the German Ministry of Education and Research (BMBF) in the framework of the R&D Program GEOTECHNOLOGIEN (Grant 03G0743B).

II. THEORY

A. Inductive coupling and pole-pole matrix

In the case of EIT measurements, two wire pairs are typically used for current injection and voltage measurement in order to obtain the transfer impedance between the two current and two potential electrodes. With a set of measured transfer impedances for different configurations, the soil conductivity can be reconstructed. In the case of EIT measurements in one borehole, the wires inside electrode chain that connect the electrodes with the EIT measurement equipment are placed parallel to each other (figure 1). The magnetic field B produced by the injecting current I_i in loop I will induce an electric voltage in loop II. This is called the mutual induction, M, between two wire pairs, and it can be calculated with [5]

$$M = \frac{\mu_0 l}{2\pi} \ln \frac{r_{14} r_{23}}{r_{13} r_{24}}, \qquad (1)$$

where r_{14}, r_{23} etc. are the radial distances between the wires and l is the common length of the wires.

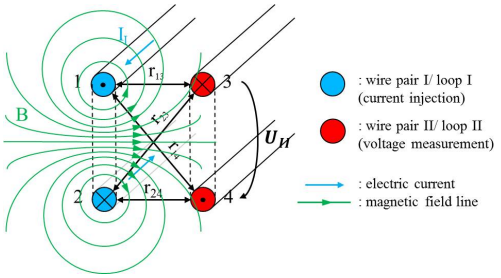

Figure 1. Mutual induction between two parallel electrical wire pairs [6].

The measured voltage U_M at loop II consists of U_0 (from the measured object) and U_{II} (induced voltage) and thus the total measured transfer impedance is given by [6]

$$Z_M = \frac{U_M}{I_I} = Z_0 + i\omega M \qquad (2)$$

This equation shows that the error due to inductive coupling can be removed by subtracting the term iωM from the measured transfer impedance.

In previous work [6], we measured the mutual inductance for all possible electrode configurations because it is practically difficult to determine the wire positions accurately. However, this is cumbersome and time-consuming. Therefore, we developed a new calibration method based on a pole-pole matrix. This pole-pole matrix was obtained using a set of pole-pole measurement (figure 2). First, we short-circuited all electrodes and connected them to the ground of the EIT system (figure 2). In each measurement, the current is injected at one electrode and it flows directly back to the ground of the EIT system. Simultaneously, the induced voltages are measured at the other seven electrodes. Then, current is injected in the next electrode and the induced voltages are measured again. This process is repeated for all eight electrodes.

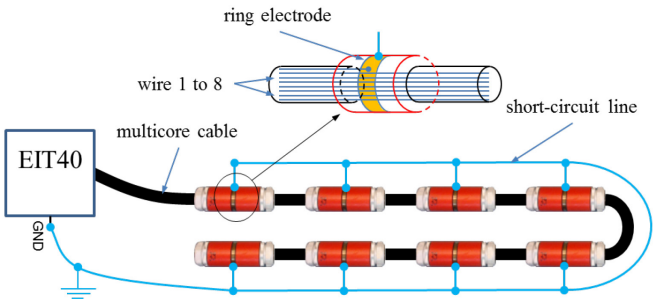

Figure 2. Pole-pole measurement for electrode chain with 8 ring electrodes and 25 m long multicore cable.

The quotient of the induced voltage and the injected current equals the mutual impedance of the two wires that were connected to the respective current and potential electrodes. Additionally, there is an additive part of the impedance from the short-circuit line (figure 2), which will cancel out in the following calculations. If electrode 1 is used as the current electrode and electrode 3 is used as the potential electrode, the transfer impedance $Z_{1,3}$ of these two wires (1 and 3) can be measured. In fact, all 56 (8x7) transfer impedances can be measured and stored in the pole-pole matrix:

$$Z_{mat} = \begin{bmatrix} 0 & Z_{1,2} & \cdots & Z_{1,7} & Z_{1,8} \\ Z_{2,1} & 0 & & Z_{2,7} & Z_{2,8} \\ \vdots & & \ddots & & \vdots \\ Z_{7,1} & Z_{7,2} & & 0 & Z_{7,8} \\ Z_{8,1} & Z_{8,2} & \cdots & Z_{8,7} & 0 \end{bmatrix}. \qquad (3)$$

Next, we set up a general equation for calculation of the mutual impedance between two wire pairs in one electrode chain with the pole-pole data:

$$\begin{aligned} Z_{C_1C_2P_1P_2} &= Z_{C_1C_2P_1} - Z_{C_1C_2P_2} \\ &= (Z_{C_2,P_1} - Z_{C_1,P_1}) - (Z_{C_2,P_2} - Z_{C_1,P_2}) \end{aligned}. \qquad (4)$$

where C1 and C2 are the numbers of current electrodes and P1 and P2 are the numbers of potential electrodes. The difference calculation in (4) eliminates the additive part from the short-circuit line. That means that there is no need to determine this part. Thus we can apply the pole-pole matrix as the calibration data for any measurement configuration the case of measurements in a single borehole. Instead of 840 measurements for all possible configurations with 8 electrodes, only 56 measurements are necessary using this newly developed pole-pole calibration.

B. Capacitive Coupling

Capacitive coupling can occur everywhere where a potential difference exists. This effect should be considered for borehole EIT measurements because of the long shielded cables. Figure 3 provides a simplified scheme that illustrates the principle of capacitive coupling. The main part of the injection current flows from the upper electrode through the conductive medium to the lower electrode. Because of the potential difference between the medium and the grounded shield, uncontrolled parasitic currents flow from the electrodes to the shield. The outer surface and the conductive shield of the cable act like small capacitors, which could considerably influence the phase accuracy of EIT measurements in the water-filled borehole [6].

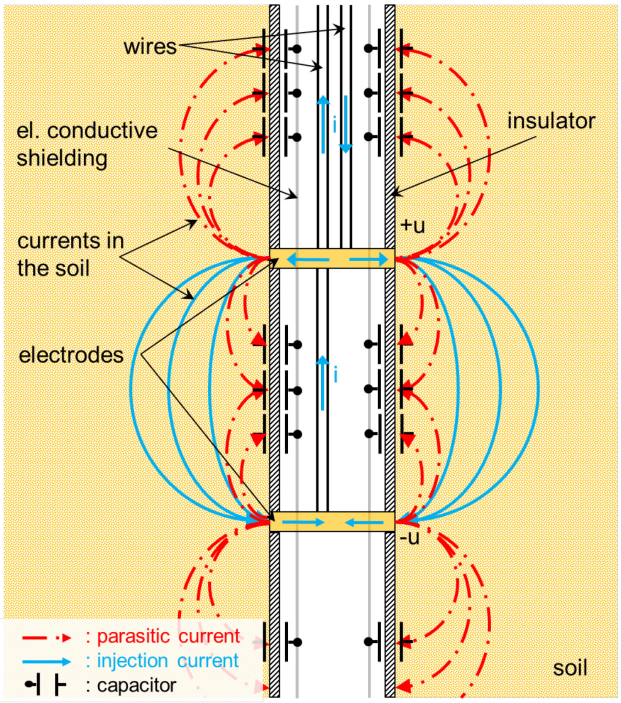

Figure 3. Capacitive coupling between the cable shield and the soil [6].

Capacitive coupling is dependent on the electrical conductivity distribution in the subsurface. However, this distribution is not known a priori, which means that the

correction for capacitive coupling is not as straightforward as the correction for inductive coupling. We considered the capacitive coupling effect by integrating discrete capacitances in the finite-element (FE) mesh of the forward electrical model used for reconstruction of the electrical conductivity distribution (figure 5). For more details about the FEM modeling we refer to [8].

III. Measurement Setup

The borehole logging tool and electrode chains were built for the field application. Both are equipped with the same dual-functionality electrode modules with integrated amplifiers for electric potential measurements and integrated switches for current injection [7]. The borehole logging tool and the electrode chain are equipped with four (16.2 cm electrode spacing) and eight electrode modules (100 cm electrode spacing), respectively. We used brass ring electrodes with a diameter of 42 mm and a height of 10 mm. The electrode modules are connected to the EIT data acquisition system with a 25 m long multicore cable (CORDIAL "CMG 16"). Each electrode is connected with one wire of the cable for the measurement. Additional wires are used for power supply and control of the electrode modules, but these wires do not influence the measurement accuracy [6].

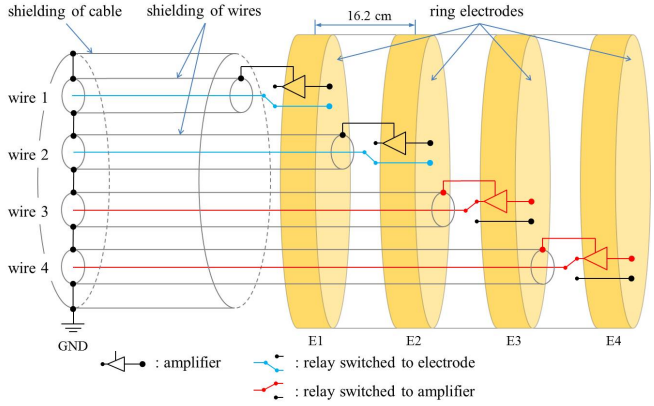

Figure 4. Simplified circuit diagram of the borehole logging tool [6].

Figure 4 provides a simplified circuit scheme for the borehole logging tool. The electrodes are numbered with 1, 2, 3 and 4, which are connected to wires inside the cable with the same numbering. In figure 4, electrodes 1 and 2 are switched to current injection and electrodes 3 and 4 are switched to potential measurement. All the shields are connected together, so that the electrode potential is measured directly against the system ground. The circuit diagram of the electrode chain with 8 electrodes is the same [6].

To verify our correction methods, we performed test measurements in a rain barrel with the borehole logging tool (4 electrodes) and used a 2D FE mesh for the forward modeling because the measurement setup is axisymmetric.

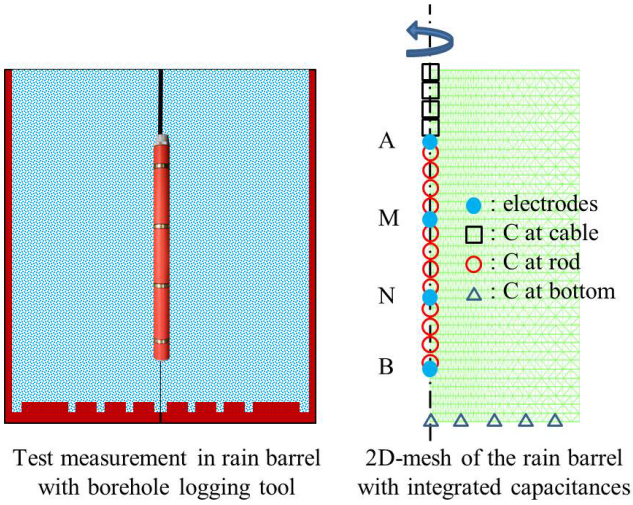

Figure 5. Modeling of the capacitive effect in the rain barrel test measurement with FEM.

Different types of capacitances were integrated into the FE mesh as shown in figure 5. For each node in the FE mesh where a capacitance is integrated, the admittance Y is calculated by

$$Y_{C_{n,n}} = i\omega C_{n,n}, \tag{5}$$

where $C_{n,n}$ is the capacitance assigned to node n of the mesh. The admittance matrix of the entire mesh is given by [6]

$$[Y_G] = [Y_S] + [Y_{C_{n,n}}], \tag{6}$$

where Y_S is the admittance matrix for the original mesh. After Ohm's law, the potential U at every node can be obtained for a given injected current I at nodes A, B. The voltage $U_{M,N}$ between two arbitrary nodes (e.g. M and N in figure 5) can be found by calculating the difference between their potentials. Thus the transfer impedance between two nodes (M and N) for a current injection at A and B can be obtained by [6]

$$Z_{M,N} = U_{M,N} \cdot I_{A,B}. \tag{7}$$

IV. Results

The results of the FEM model applied to the rain barrel test measurement are compared with the transfer impedance corrected for inductive coupling in figure 6. It can be seen that there is an excellent agreement for the imaginary part and the phase angle of the modeled transfer impedances Z_C and the impedances after correction of inductive coupling Z_{cr}. The small deviation of about 0.7 Ω for the real part of the transfer impedance is related to geometry errors in the FE modeling. After considering both coupling effects, we obtained a phase accuracy of 0.8 mrad at 10 kHz for the rain barrel measurements.

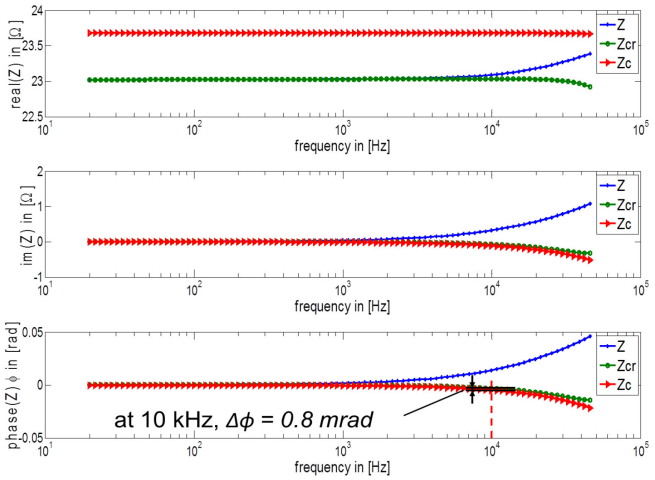

Figure 6. The spectrum of original measured transfer impedances Z, inductive corrected data Zcr, and modeled data Zc.

In a final step, we applied the correction methods to field measurements made with the borehole electrode chain (8 electrodes) and reconstructed the complex resistivity of the soil using the originally measured impedance, the impedance after correction of inductive coupling and the modeled impedance due to the capacitive coupling (figure 7). The inversion of the uncorrected measurements resulted in relatively large phase values that even included physically implausible positive values for some depths. After the correction for inductive coupling, lower and entirely negative phase values were obtained. It can be seen that the two inversion results differ considerably, with differences of up to 10 mrad. The consideration of capacitive coupling resulted in a positive phase shift for the entire profile with a maximum of 3 mrad at 2 m depth. As expected, the inversion results for the real part of the resistivity were not affected by the correction procedures.

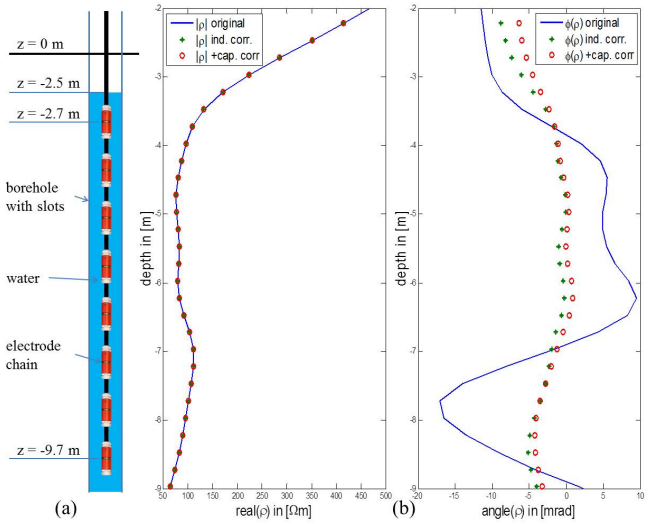

Figure 7. (a) Measurement setup, (b) Reconstructed real component and phase angle of the complex resistivity against depth at 1kHz for the raw EIT measurements, the EIT measurements after correction for inductive coupling, and the modeled impedances with integrated capacitances [6].

V. Conclusion

We presented correction approaches for inductive coupling between the current and the potential loops inside a multicore cable and capacitive coupling between the cable and the electrically conductive environment in EIT measurements. In order to verify these correction approaches, we performed EIT measurements in a rain barrel filled with water using a borehole EIT logging tool. For these controlled conditions, a high phase accuracy of about 0.8 mrad at 10 kHz was achieved. The results show that we achieved the same accuracy using the pole-pole calibration method as with the more laborious method presented in [6]. Additionally, we performed borehole EIT measurements at the Krauthausen test site using a borehole electrode chain to demonstrate the improvements achieved by the correction approaches. Inverted resistivity magnitude and phase profiles considering both corrections matched well with the general stratigraphy of the test site [3].

References

[1] Binley A, Slater L D, Fukes M and Cassiani G 2005 Relationship between spectral induced polarization and hydraulic properties of saturated and unsaturated sandstone Water Resour. Res. vol 41 p W12417

[2] Kemna A, Binley A, Ramirez A and Daily W 2000 Complex resistivity tomography for environmental applications Chem. Eng. J. vol 77 pp 11 - 8

[3] Kemna A, Kulessa B and Vereecken H 2002 Imaging and characterisation of subsurface solute transport using electrical resistivity tomography (ERT) and equivalent transport models J. Hydrol. vol 267 pp 125-46

[4] Kemna A, Huisman J A, Zimmermann E and Fechner T 2011 4D Spectral Electrical Impedance Tomography GEOTECHNOLOGIEN Science Report (Potsdam, GEOTECHNOLOGIEN) DOI 10.2312/GFZ.gt.18.06

[5] Küpfmüller K E h, Mathis W and Reibiger A 2008 Theoretische Elektrotechnik (Berlin/Heidelberg, Springer)

[6] Zhao Y, Zimmermann E, Huisman J A, Treichel A, Wolters B, Waasen S v and Kemna A 2013 Broadband EIT borehole measurements with high phase accuracy using numerical corrections of electromagnetic coupling effects Measurement Science and Technology vol 24 p 085005

[7] Zimmermann E, Kemna A, Berwix J, Glaas W and Vereecken H 2008 EIT measurement system with high phase accuracy for the imaging of spectral induced polarization properties of soils and sediments Meas. Sci. Technol. vol 19 p 094010

[8] Zimmermann E 2011 Phasengenaue Impedanz-spektroskopie und -tomographie für geophysikalische Anwendungen PhD thesis (Rheinische Friedrich-Wilhelms-Universität Bonn)